Thermal stresses in surface-coated Fe-3%Si sheet

L. CENIGA
Institute of Materials Research, Watsonova 47, 043 53 Košice, Slovak Republic
E-mail: ceniga@saske.sk

The aim of the paper is to present a model of thermal stresses in a layered plane system, and consequently to verify the model validity by comparing calculated thermal stresses with measured thermal stresses. The paper deals thus with thermal stresses in the Fe-3%Si sheet for magnetic applications, having a surface coating of the $2MgO{\cdot}TiO_2$, ZrO_2, TiO_2, Al_2O_3, $2MgO{\cdot}SiO_2$, $MgO{\cdot}Al_2O_3$ oxides. The thermal stresses, originating during a cooling process as a consequence of the difference in thermal expansion coefficients between the Fe-3%Si sheet and the surface coating, degrade hysteresis losses of the Fe-3%Si sheet. Magnetic properties of the presented coating–Fe-3%Si systems, as the magnetic induction and the hysteresis losses before and after coating formation, are presented. The theoretical background, including the model of the thermal stresses in anisotropic and isotropic two-layered plane systems, consequently transformated to the three-layered plane system, is presented. Calculated thermal stresses are compared with those of a tension measurement of the presented coating—Fe-3%Si systems, numerical equality of the calculated and measured thermal stresses is observed.

1. Introduction

As the consequence of the difference in the thermal expansion coefficients between the individual layers, the thermal stresses originate during the cooling process in the layered system to cool down from the initial temperature, T_i, to the final temperature, T_f.

The presented calculation of the thermal stresses is performed for the anisotropic and isotropic two-layered plane system (A/B) (Fig. 1), using the transformation to the anisotropic and isotropic three-layered plane system ($A/B/A$). The thermal stresses are derived on the basis of the following premises:

1. The thermal expansion and elastic coefficients, α_{1Q}, α_{jQ} and s_{2jQ}, s_{3jQ}, respectively, along the axis x_{jQ} ($j = 2, 3$) of the Cartesian system ($0x_{1Q}x_{2Q}x_{3Q}$) (Fig. 1), the Young's modulus, E_Q, the Poisson's number, μ_Q, of the layer $Q(Q = A, B)$ are temperature-independent in the temperature range, $\langle T_f, T_i\rangle$, of the cooling process [1]. During the cooling process, no microstructural changes occur [1].

2. The Hooke's laws (3), (4), (9) [2] are valid in whole temperature range of the cooling process without consideration of the high-temperature stress relaxation [1]. In regard to the A/B configuration (Fig. 1), the A/B system may be assumed not to be acted by the stress σ_{11Q} [2].

2. Theoretical background

2.1. Anisotropic two-layered plane system

Fig. 1 shows the A/B system of which dimensions at the temperature $T \in \langle T_f, T_i\rangle$, t_{QT} and l_{jQT} for $x_{1Q} = 0$, along the axes x_{1Q} and x_{jQ} ($j = 2, 3$; $Q = A, B$) of the Cartesian system ($0x_{1Q}x_{2Q}x_{3Q}$), respectively, can be written in the forms

$$t_{QT} = t_{Qf}[1 + \alpha_{1Q}(T - T_f)], \tag{1}$$

$$l_{jQT} = l_{ji}[1 - \alpha_{jQ}(T_i - T)], \tag{2}$$

where t_{Qf} and l_{ji} are the thickness of the layer Q and the A/B system dimension along the axis x_{jQ} at the temperature T_f and T_i, respectively (Fig. 1).

During the cooling process, the A/B system plane $x_{2Q}x_{3Q}$ for $x_{1Q} = 0$ may be assumed to represent the zero-stress plane. In the case that $\alpha_{jA} < \alpha_{jB}$, the layers A and B are acted by the compressive and tensile stresses, respectively, and the A/B system may be thus assumed to exhibit the shape shown in Fig. 2. The x_1-dependences of the strain ε_{jjQ}, and consequently of the stress σ_{jjQ} ($j = 2, 3$) acting in the layer $Q(Q = A, B)$ for $x_{1Q} \in \langle 0, t_{QT}\rangle$, have the forms

$$\varepsilon_{jjA} = s_{2jA}\sigma_{22A} + s_{3jA}\sigma_{33A} = \frac{l_{jAT}(x_{1A}) - l_{jAT}}{l_{jAT}} = -c_{jA}x_{1A}, \tag{3}$$

$$\varepsilon_{jjB} = s_{2jB}\sigma_{22B} + s_{3jB}\sigma_{33B} = \frac{l_{jBT}(x_{1B}) - l_{jBT}}{l_{jBT}} = c_{jB}x_{1B}, \tag{4}$$

$$\sigma_{22A} = -\frac{c_{23A}x_{1A}}{t_{AT} + t_{BT}}, \tag{5}$$

$$\sigma_{33A} = -\frac{c_{32A}x_{1A}}{t_{AT} + t_{BT}}, \tag{6}$$

$x_{1B} \in \langle t_B/2, t_B \rangle$, and is thus determined by (7)–(12), using the transformation $t_{Bf} \rightarrow t_{Bf}/2$ in (1).

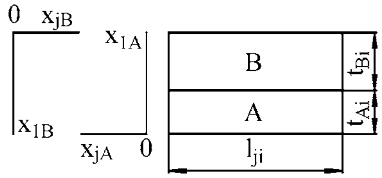

Figure 1 The two-layered plane system (A/B) of the thickness of the layer Q, t_{Qi}, and of the dimension along the axis x_{jQ} ($j = 2, 3$; $Q = A, B$) of the Cartesian system ($0x_{1Q}x_{2Q}x_{3Q}$), l_{ji}, at the temperature T_i of the cooling process of the temperature range $\langle T_i, T_f \rangle$, where T_i is the initial temperature and T_f is the final temperature. The A/B system plane for $x_{1Q} = 0$ may be assumed to represent the zero-stress plane.

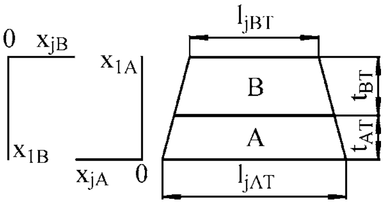

Figure 2 The two-layered plane system (A/B) of the thickness of the layer Q, t_{QT} (1), and of the dimension along the axis x_{jQ} ($j = 2, 3$; $Q = A, B$) of the Cartesian system ($0x_{1Q}x_{2Q}x_{3Q}$), l_{jQT} (2), at the temperature $T \in \langle T_i, T_f \rangle$, where T_i is the initial temperature and T_f is the final temperature of the cooling process. The A/B system plane for $x_{1Q} = 0$ may be assumed to represent the zero-stress plane.

$$\sigma_{22B} = \frac{c_{23B} x_{1B}}{t_{AT} + t_{BT}}, \tag{7}$$

$$\sigma_{33B} = \frac{c_{32B} x_{1B}}{t_{AT} + t_{BT}}, \tag{8}$$

$$c_{23Q} = \frac{c_{2Q} s_{33Q} - c_{3Q} s_{23Q}}{s_{22Q} s_{33Q} - s_{23Q}^2}, \tag{9}$$

$$c_{32Q} = \frac{c_{3Q} s_{22Q} - c_{2Q} s_{23Q}}{s_{22Q} s_{33Q} - s_{23Q}^2}, \tag{10}$$

$$c_{jQ} = \frac{(\alpha_{jB} - \alpha_{jA})(T_i - T)}{(t_{AT} + t_{BT})[1 - \alpha_{jQ}(T_i - T)]}, \tag{11}$$

$$j = 2, 3, \quad Q = A, B.$$

Considering the influence of σ_{jjQ} ($j = 2, 3$; $Q = A, B$) on the layer thickness, the thickness t_{QT} in (5)–(11) may be replaced by

$$\begin{aligned} t_Q &= t_{QT} - \int_0^{t_{QT}} \varepsilon_{11Q}\, dx_{1Q} \\ &= t_{QT} - \int_0^{t_{QT}} (s_{12Q}\sigma_{22Q} + s_{13Q}\sigma_{33Q})\, dx_{1Q} \\ &= t_{QT}\left[1 + t_{QT}\frac{(\delta_{QA} - \delta_{QB})(s_{12Q}c_{23Q} + s_{13Q}c_{32Q})}{2(t_{AT} + t_{BT})}\right], \end{aligned} \tag{12}$$

where δ_{QA}, δ_{QB} are the Kronecker's symbols.

In the $A/B/A$ system of the thickness t_A, t_B, t_A of the individual layers, the planes $x_{2A}x_{3A}$ and $x_{2B}x_{3B}$ for $x_{1A} = 0$ and $x_{1B} = t_B/2$, respectively, may be assumed to represent the zero-stress planes. The stress σ_{jjB} ($j = 2, 3$) in the $A/B/A$ system exhibits the symmetrical x_1-dependences within the intervals $x_{1B} \in \langle 0, t_B/2 \rangle$, $x_{1B} \in \langle t_B/2, t_B \rangle$, and is thus determined by (7)–(12), using the transformation $t_{Bf} \rightarrow t_{Bf}/2$ in (1).

2.2. Isotropic two-layered plane system

Using the transformations $\alpha_{1Q}, \alpha_{jQ} \rightarrow \alpha_Q$; $s_{jjQ} \rightarrow 1/E_Q$; $s_{12Q}, s_{13Q}, s_{23Q} \rightarrow -\mu_Q/E_Q$, the stress $\sigma_Q = \sigma_{jjQ}$ ($j = 2, 3$), acting in the plane $x_{2Q}x_{3Q}$ of the layer $Q(Q = A, B)$ of the isotropic A/B system for $x_{1Q} \in \langle 0, t_Q \rangle$, has the forms

$$\sigma_A = \sigma_{jjA} = -\frac{c_A x_{1A}}{t_A + t_B}, \quad j = 2, 3, \tag{13}$$

$$\sigma_B = \sigma_{jjB} = \frac{c_B x_{1B}}{t_A + t_B}, \quad j = 2, 3, \tag{14}$$

$$t_Q = t_{QT}\left[1 + t_{QT}\frac{\mu_Q c_Q(\delta_{QA} - \delta_{QB})}{E_Q(t_{AT} + t_{BT})}\right], \quad Q = A, B, \tag{15}$$

$$c_Q = \frac{E_Q(\alpha_B - \alpha_A)(T_i - T)}{(1 - \mu_Q)[1 - \alpha_Q(T_i - T)]}, \quad Q = A, B. \tag{16}$$

3. Thermal stresses in surface-coated Fe-3%Si sheet

The Fe-3%Si sheet [wt%], representing the steel for magnetic applications, is used as a material for magnetic cores. Applying the surface coating of suitable adhesion to the Fe-3%Si sheet surface, and of the thermal expansion coefficient less than the Fe-3%Si sheet, the Fe-3%Si sheet is acted by the tensile stresses to degrade the hysteresis losses of the Fe-3%Si sheet [3–7]. To achieve high tensile stresses, the layered system has to exhibit the differential of the thermal expansion coefficients of the individual layers of not less than $6 \times 10^{-6}\,K^{-1}$ [3, 4, 7]. Material constants of the Fe-3%Si sheet [8] and of the surface coatings [7] applied to the Fe-3%Si sheet are listed in Table I. In regard to the thermal expansion coefficients and Section 2.2, the surface coating and the Fe-3%Si sheet represent the layers A_n ($n = 1$–6) and B of the isotropic two-layered plane system, respectively.

Temperature dependences of the compressive and tensile stresses, σ_A and σ_B, acting in the layers A_n and B on the $A_n - B$ boundary of the A_n/B system (Figs 1 and 2), cooling down from the initial temperature, $T_i = 550°C$, to the final temperature, $T_f = 20°C$, are shown in Fig. 3, respectively. The temperature of 550°C represents the minimum temperature of a relaxation process of the coating—Fe-3%Si system [9]. Due to the coating—Fe-3%Si isotropy, the stresses σ_A and σ_B in the layers A_n and B of the thickness at the final temperature, $t_{Af} = 3\ \mu m$ and $t_{Bf} = 0.2$ mm (1), are determined by (1), (13)–(16), for $x_{1A} = t_A$ and $x_{1B} = t_B$ (1), (15) and (16), respectively.

Considering the influence of the acting thermal stresses on the layer thickness (15), (16), Table I presents calculated thermal stresses at the final temperature of the cooling process, σ_{Af}, σ_{Bf} (1), (13)–(16), and the measured stress, σ_{Bfm}, determined by Kanai *et al.*

TABLE I The material constants of the surface coatings [7] and the Fe-3%Si sheet [8, 9]. The calculated thermal stresses, σ_{Af}, σ_{Bf} (Fig. 3) for $x_{1A} = t_A$, $x_{1B} = t_B$ (1), (15) and (16), respectively, and the measured thermal stress, σ_{Bfm} for $x_{1B} = t_B$, acting in the surface coating (A_n) and the Fe-3%Si sheet (B) on the coating—Fe-3%Si boundary (Figs 1 and 2), are determined by (1), (13–16), and by the tension measurement by Kanai *et al.* [7], respectively, at the final temperature of the cooling process, T_f. The calculated thermal stresses, σ_{Af}, σ_{Bf}, are determined on the following conditions [7]: the initial and final temperature of the cooling process, $T_i = 550°C$ and $T_f = 20°C$, respectively; the thickness of the surface coating and of the Fe-3%Si sheet at the final temperature, $t_{Af} = 3\ \mu m$ and $t_{Bf} = 0.2$ mm (1), respectively; the temperature of 550°C represents the minimum temperature of the relaxation process of the coating–Fe-3%Si system [9–11]. The magnetic induction of the Fe-3%Si sheet at the magnetic field intensity of 800 Am^{-1}, B_8 [7], and the hysteresis losses of the Fe-3%Si sheet at the magnetic induction of 1.7 T and at the frequency of 50 Hz, $W_{17/50}$ [7], both before/after the coating formation, along with the decrease of the hysteresis losses in [%] after the coating formation, are presented

n	Coating (Layer A_n)	E_A (GPa)	μ_A	α_A ($10^{-6}\ K^{-1}$)	σ_{Af} (MPa)	σ_{Bf} (GPa)	σ_{Bfm} (GPa)	B_8^a (T)	$W_{17/50}^b$ ($W\ kg^{-1}$)
1	$2MgO{\cdot}TiO_2$	20		2.0	−1.6	1.08	1.0	1.939/1.920	0.82/0.67/18%
2	ZrO_2	140		1.1	−16.2	1.13	1.1	1.939/1.921	0.83/0.67/19%
3	TiO_2	290	0.25	4.4	−21.8	1.15	1.2	1.937/1.924	0.81/0.65/20%
4	Al_2O_3	400		3.2	−24.2	1.17	1.2	1.938/1.921	0.82/0.65/21%
5	$2MgO{\cdot}SiO_2$	220		1.0	−26.5	1.22	1.2	1.936/1.916	0.82/0.65/21%
6	$MgO{\cdot}Al_2O_3$	250		3.6	−30.6	1.27	1.4	1.935/1.917	0.83/0.64/23%
	Sheet (Layer B)	E_B (GPa)	μ_B	α_B ($10^{-6}\ K^{-1}$)					
	Fe-3%Si	225	0.23	11.7					

[a]Before/after coating formation.
[b]Before/after coating formation/decrease of hysteresis losses in (%).

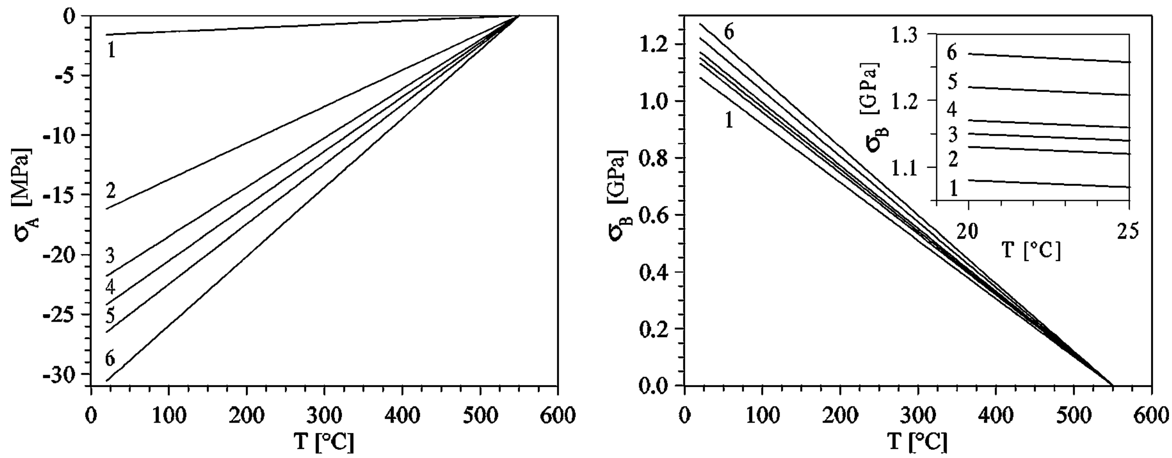

Figure 3 Temperature dependences of the compressive and tensile stresses, σ_A for $x_{1A} = t_A$ and σ_B for $x_{1B} = t_B$ (1), (13)–(16), acting in the layers A_n and B on the $A_n - B$ boundary of the A_n/B system (Figs 1 and 2), cooling down from the initial temperature, $T_i = 550°C$, to the final temperature, $T_f = 20°C$. The temperature of 550°C represents the minimum temperature of the relaxation process of the coating—Fe-3%Si system [9–11]. The layers A_n (n = 1–6) and B of the thickness at the final temperature, $t_{Af} = 3\ \mu m$ and $t_{Bf} = 0.2$ mm [7], are represented by the surface coating and the Fe-3%Si sheet (Table I), respectively.

[7] by the tension measurement at the final temperature of the cooling process, T_f, and on the above conditions, $T_i = 550°C$, $T_f = 20°C$, $t_{Af} = 3\ \mu m$, $t_{Bf} = 0.2$ mm (1), $x_{1A} = t_A$, $x_{1B} = t_B$ (1), (15), (16). The calculated and measured thermal stresses (Table I) are influenced by the thermal expansion coefficients, α_A and α_B, as well as by the Young's moduli of the coatings and the Fe-3%Si sheet (13)–(16), E_A and E_B, respectively, as presented in [3, 7]. In regard to the premises (1), (2), the differences between σ_{Bf} and σ_{Bfm} are probably caused by the temperature dependence of the material constants of the surface coatings and the Fe-3%Si sheet, and by the high-temperature stress relaxation.

The magnetic induction of the Fe-3%Si sheet at the magnetic field intensity of 800 Am^{-1}, B_8 [7], and the hysteresis losses of the Fe-3%Si sheet at the magnetic induction of 1.7 T and at the frequency of 50 Hz, $W_{17/50}$ [7], both before/after the coating formation, along with the decrease of the hysteresis losses in [%] after the coating formation, are listed in Table I. After the coating formation, the hysteresis losses of the Fe-3%Si sheet of the presented coating–Fe-3%Si systems exhibit the decrease up to 18–23%, following the increase of the calculated and measured [7] thermal stresses acting on the coating–Fe-3%Si boundary. As presented in Table I, more considerable decrease of the hysteresis losses of the Fe-3%Si is related to higher thermal stress (Table I) [7], however, this observed result might not be assumed to be generally valid.

4. Conclusions

The results of the presented calculation of the thermal stresses, acting in the Fe-3%Si sheet for magnetic applications, surface-coated by the $2MgO{\cdot}TiO_2$, ZrO_2, TiO_2, Al_2O_3, $2MgO{\cdot}SiO_2$, $MgO{\cdot}Al_2O_3$ oxides, originating during the cooling process as the consequence of the difference in the thermal expansion coefficients between the Fe-3%Si sheet and the surface coating, and degrading the hysteresis losses of the Fe-3%Si sheet, are as follows:

1. The formulae for the thermal stresses, (5)–(11) and (13)–(16), and the formulae for the layer thickness influenced by the thermal stresses, (12) and (15), for the anisotropic and isotropic two-layered plane system, respectively, are presented.

2. The transformation of the thermal stresses of the two-layered plane system (A/B) to the three-layered plane system ($A/B/A$) is presented.

3. The temperature dependences of the thermal stresses acting in the Fe-3%Si sheet and in the surface coating on the coating—Fe-3%Si boundary are presented (Fig. 3). The calculated thermal stresses are determined by the derived formulae (13)–(16), and compared with those determined by the tension measurement by Kanai *et al*. (Table I) [7]. The calculated and measured values (Table I) are influenced by the thermal expansion coefficients as well as by the Young's moduli of the coatings and the Fe-3%Si sheet (13)–(16) as presented in [3, 7]. Numerical equality of the calculated and measured thermal stresses is observed.

4. The magnetic induction of the Fe-3%Si sheet at the magnetic field intensity of 800 Am^{-1} [7], and the hysteresis losses of the Fe-3%Si sheet at the magnetic induction of 1.7 T and at the frequency of 50 Hz [7], both before/after the coating formation, along with the decrease of the hysteresis losses are presented. After the coating formation, the hysteresis losses of the Fe-3%Si sheet of the presented coating—Fe-3%Si systems exhibit the decrease up to 18–23%, following the increase of the measured [7] and calculated thermal stresses acting on the coating–Fe-3%Si boundary (Table I).

Acknowledgements
This work was supported by the Slovak Grant Agency VEGA (2/1063/21, 2/1145/21).

References
1. T. MIZUTANI, *J. Mater. Res.* **11** (1996) 483.
2. R. F. S. HEARMON, in "Introduction to Applied Anisotropic Elasticity" (The Clarendon Press, Oxford, 1961) p. 18.
3. T. JOMAMOTO, *IEEE Trans. Magn.* **8** (1972) 677.
4. V. HAJKO, L. POTOCKÝ and A. ZENTKO, in "Magnetization Processes" (Alfa, Bratislava, Slovak Republic, 1982) p. 225.
5. F. J. G. LANDGRAF, M. EMURA, K. ITO and P. S. G. CARVALHO, *J. Magn. Magn. Mater* **215** (2000) 94.
6. V. E. IORDACHE, F. OSSART and E. HUG, *ibid.* **254** (2003) 57.
7. T. KANAI, K. TANEMOTO, S. YAMAZAKI and T. NAGASHIMA, United States Patent. Number 5,411,808 (1995).
8. J. MIKULČÁK, L. KRKAVEC, B. KLIMEŠ, J. BARTŮNĚK, J. ŠIROKÝ and M. PAUKOVÁ, in "Tables on Mathematics, Physics and Chemistry" (SPN, Bratislava, Slovak Republic, 1966) p. 239.
9. P. SKOČOVSKÝ, O. BOKŮVKA, R. KONEČNÁ and E. TILLOVÁ, in "Science on Materials for Mechanical Engineers" (EDIS Technical University in Žilina, Slovak Republic, 2001) p. 252 (in Slovak).
10. Y. SIDOR and F. KOVÁČ, *Metalurgija* **42** (2003) 153.
11. J. JANOVEC, A. VÝROSTKOVÁ and M. SVOBODA, *Metall. Mater. Trans.* A **25** (1994) 267.

Received 25 February
and accepted 23 June 2003